

1 Estimations of soil metal accumulation or leaching potentials under climate change scenarios: the Example of
2 copper on a European scale

3

4 Laura SERENI^{1,2}, Julie-Maï PARIS³, Isabelle LAMY¹, Bertrand GUENET³

5 ¹Université Paris-Saclay, INRAE, AgroParisTech, UMR EcoSys, 91120 Palaiseau, France

6 ²Present address: Univ. Grenoble Alpes, CNRS, INRAE, IRD, Grenoble INP, IGE, Grenoble, France

7 ³Laboratoire de Géologie ENS, PSL Research University, CNRS, UMR 8538, IPSL, Paris, France

8 *Correspondence to Laura Sereni (laurasereni@yahoo.fr)

9

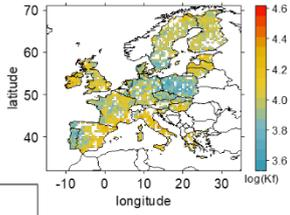
10 Abstract:

11 Contaminants inputs to soil are highly dependent on anthropogenic activities while contaminant
12 retention, mobility and availability are highly dependent on soil properties. The knowledge of partitioning
13 between soil solid and solution phases is necessary to estimate whether deposited amounts of contaminants will
14 rather be transported with runoff or accumulated. Besides, runoff is expected to change during the next
15 century due to changes in climate and in rainfall patterns. In this study, we aimed at estimating at the European
16 scale the areas with a potential risk due to contaminant leaching (LP). We also defined in the same way the
17 surface areas where limited Cu leaching occurred, leading to potential accumulation (AP) areas. We focused
18 on copper (Cu) widely used in agriculture under mineral form or associated to organic fertilizers, resulting in high
19 spatial variations in deposited and incorporated amounts in soils as well than in European policies of application.
20 We developed a method using both Cu partition coefficients (K_f) between total and dissolved Cu forms, and runoff
21 simulation results for historical and future climates. The calculation of K_f with pedo-transfer functions allowed us
22 to avoid any uncertainties due to past management or future depositions that may affect total Cu concentrations.
23 Areas with high potential risk of leaching or of accumulation were estimated over the 21st century by

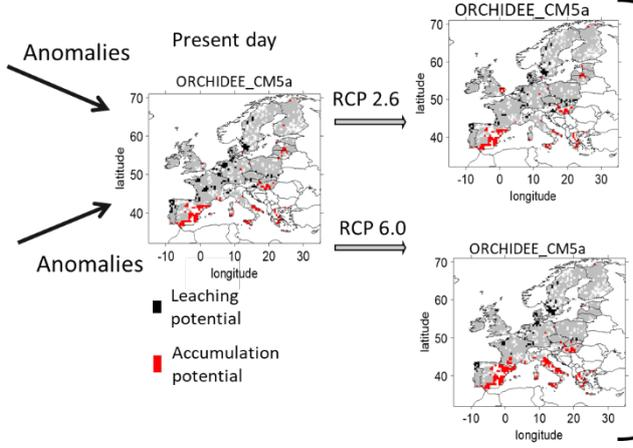
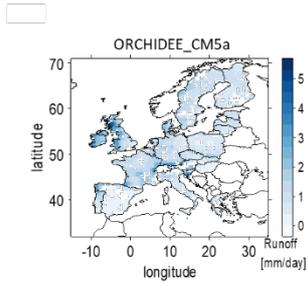
24 comparing K_f and runoff to their respective European median. Thus, at three distinct times, we considered a grid
25 cell at risk of LP if its K_f was low compared to the European median and its runoff was high compared to the
26 European median of the time. Similarly, a grid cell was considered at risk of AP if its K_f was high and its runoff was
27 low compared to their respective European median of the time. To deal with uncertainties in climate change
28 scenarios and the associated model prediction, we performed our study with two representative atmospheric
29 greenhouse gases concentration pathways (RCP), defined with climate change associated to a large set of socio-
30 economic scenarios found in the literature. We used two land surface models (ORCHIDEE and LPJmL, given soil
31 hydrologic properties) and two global circulation models (ESM2m and CM5a, given rainfall forecast). Our results
32 show that, for historical scenario 6.4 ± 0.1 % (median, median deviation) and 6.7 ± 1.1 % of the grid cells of the
33 European land surfaces are with LP and AP respectively. Interestingly, our results simulate a constant global
34 surface with by LP and AP, around 13% of the grid cells, consistent with an increase in AP and a decrease in LP.
35 Despite large variations in LP and AP extents depending on the land surface model used for estimations, the two
36 trends were more pronounced with RCP 6.0 than with RCP 2.6, highlighting the global risk of combined climate
37 change and contamination and the need for more local and seasonal assessment. Results are discussed to
38 highlight the points requiring improvement to refine predictions.

39 Keywords: regional modeling, transfer functions, ISIMIP, LUCAS Topsoil data, mapping risk

$$K_f = \frac{Cu_{total}}{Cu_{solution}} \text{ computation}$$



Runoffs
predicted by
models



X
2 Global Circulation
Models
2 Land Surface
Models

40

41

42

43 1. Introduction

44

45 At a large spatial scale, trace element contents in soils are highly variable in relation with the trace element
46 contents of the soil parental rocks and with local anthropogenic inputs of various origins (Flemming and Trevors,
47 1989; Salminen and Gregorauskiene, 2000; Noll, 2003). Some trace elements like copper (Cu) or zinc are required
48 for several biological mechanisms, but when highly concentrated they may have toxic effects on soil organisms
49 (Giller et al., 1998). In particular, Cu is widely used as a fungicide, especially against downy mildew in vineyard
50 parcels (Komárek et al., 2010), but also in industrial processes. Besides, Cu application to soils are numerous, in
51 the mineral form or within the organic fertilizers applied, leading to a global European limit of application. At the
52 European scale, a gradient of soil Cu concentrations can be found from typical baseline values between 5 mgCu.kg^{-1}
53 to 20 mgCu.kg^{-1} (Salminen and Gregorauskiene, 2000), to values larger than 100 mgCu.kg^{-1} , common in cultivated
54 soils and especially in vineyards parcels (Ballabio et al., 2018). It is commonly accepted to conceptually partition
55 the total soil Cu content into different pools of Cu forms in close equilibrium. Briefly, three pools can be defined:
56 a so-called 'inert' pool corresponding to Cu included into minerals, a so-called 'labile' pool corresponding to Cu
57 sorbed to soil constituents but that can be mobilized according to environmental conditions, and a smallest
58 'mobile' pool corresponding to Cu in soil solution that may be readily available for living organisms but also for
59 transport within soil horizons (West and Coombs, 1981; Rooney et al., 2006; Broos et al., 2007). Schematically,
60 these pools are governed by processes like exchange, complexation or sorption. Also, local soil characteristics
61 such as organic matter, pH or cationic exchange capacity can affect the proportion of Cu in these different pools
62 (Vidal et al., 2009). Any modifications in soil properties or soil solution composition may thus affect Cu equilibrium
63 between sorbed and solution phases. The pool of Cu in the solution phase can be assimilated to a potential pool
64 of Cu leaching. Conversely, Cu bound to the solid phases can be assimilated to a potential pool of Cu accumulation
65 in soil. Depending on the main process involved, for a given amount of Cu deposited on soil, the proportions of
66 leached and accumulated Cu can vary from place to place and with time. However, studies simulating whether
67 the soil will rather leach or accumulate a contaminant are scarce especially at a large spatial scale. Know and

68 predict this leaching or retention, however, could allow to highlight contaminated areas with a potential to leach,
69 disperse or accumulate contaminants, and therefore help for long term environmental management.

70 Concurrently, climate change due to anthropogenic activities is expected to impact rainfall patterns in the
71 forthcoming decades, leading to changes in the frequency and intensity of weather events at regional and local
72 levels (Christensen and Christensen, 2003). For instance, an increase in rain- and snow-fall events in winter in
73 Northern Europe but a decrease in summer in the Mediterranean region are projected, which extends to
74 northward regions (Douville et al., 2021) with extent of rain- and snow-fall alterations depending on climate
75 change. Thus, climate change will alter the soil waterflows throughout the century (Mimikou et al., 2000). For
76 instance, increase in rainfall intensity and in water accumulation in the soil surface due to limited water infiltration
77 may induce large runoff (Chu et al., 2019). Changes in runoff will also change fluxes of elements or of particulates
78 in the soil solution as it has been shown for Cu (Babcsányi et al., 2016). However, predicting how these runoff
79 changes will relate to elemental contaminant fluxes in the coming decades remain difficult.

80 In this framework, our aim was twofold: i) estimate the areas the most likely to lose soil Cu within soil solution
81 and waterflows, thereafter named leaching potential areas [LP], for the historical period (2001-2005)
82 and ii) predict their changes according to different climate change scenarios. Additionally, we aimed to estimate
83 the areas the most likely to accumulate Cu, thereafter named accumulation potential areas [AP]. We
84 hypothesized that the processes of Cu accumulation or leaching can be described by the combined effects
85 of local runoff amounts and of local soil properties controlling the partition of total Cu in sorbed and solution
86 species. Due to the lack of information about the future Cu deposition whatever its form, we developed a
87 method using the partition coefficient (K_f) at the equilibrium between solid and solution phases to determine
88 areas with high or low potential of leaching whatever total Cu concentration. Regarding the lack of data about
89 future deposited amounts at large scale, using K_f was necessary to estimate the Cu mobility potential. The LP
90 or AP areas were thus estimated through the combined use of K_f , calculated with the help of pedo-transfer
91 functions, and the use of soil runoff amounts extracted from earth system simulations. With the use of K_f we

92 avoided the uncertainties due to past land management and previous Cu deposition and focused on risks arising
93 from future deposition. To do so, we first reviewed the empirical equations estimating Cu's K_f based on soil
94 properties to highlight generic soil properties governing this partition. From this review, we extracted the best
95 compromise K_f equation to estimate partitioning at the regional scale, which ensures more accurate K_f calculation
96 based on pedo-geochemical data typically recorded in soil surveys, thus mainly available. This allowed us to
97 estimate Cu's K_f values to be used at the European scale based on pedo-geochemical soil surveys without the
98 knowledge of soil Cu total content. We then focused on the current state of the climate and its projected changes
99 over the 21st century, based on two climate change scenarios. The rainfall predictions were analyzed at the
100 0.5° that is a common scale for land surface models allowing a multi-comparison to capture the
101 variability in soil properties and rainfall regime. To capture the difficulties in runoff prediction and to disentangle
102 the uncertainties between rainfall prediction and runoff calculations of land surface models, we used a set of
103 simulations provided by the Inter-Sectoral Impact Model Intercomparison Project (ISIMIP). These simulations
104 used different land surface models driven by different climate forcings computed by different climate models. For
105 each scenario and each couple of land surface model and climate forcing we estimated the LP or AP of each grid
106 cells by comparison between the local values of K_f and of runoff to the respective calculated European median
107 that is less driven by extreme than mean.

108

109 2. Materials and methods

110

111 2.1. Equations to estimate copper K_f

112 The rigorous definition of K_f is based on the concentration ratio of sorbed vs solution species (here Cu) at the
113 equilibrium. Yet, for practical reasons of measurement and applicability, K_f is conventionally derived from total Cu
114 and not from sorbed Cu (Degryse et al., 2009). A general form of the Cu partition coefficient between soil and
115 solution – K_f – can be used to describe Cu concentrations in the sorbed and solution phases, defined as Eq. (1):

116

$$117 \quad K_f = \frac{Cu_{total}}{Cu_{solution}^n} \quad (1)$$

118 Where Cu_{total} is the total Cu content of soil in $mg.kg^{-1}$, $Cu_{solution}$ is the Cu content of soil solution in $mg.L^{-1}$ and n
119 stands for the variation in binding strength with metal loading (Groenenberg et al., 2010). A low K_f reflects a high
120 proportion of Cu in solution for a given total Cu content of the soil. K_f can vary as a function of different soil
121 parameters (Degryse et al., 2009; Elzinga et al., 1999) and can also be estimated using Eq. (2):

$$122 \quad (K_f) = a_0 + \sum_i a_i \log_{10}(X_i) \quad (2)$$

123 with X_i the different soil parameters and a_i the corresponding associated coefficient to the parameter.

124 Numerous studies in the literature have attempted the determination of the value of K_f using the Eq. (2) based
125 on statistical relationships between soil pedo-geochemical parameters, Cu in solution and total Cu measurements.
126 The soil pedo-geochemical parameter X_i and its associated coefficient a_i can differ depending on the study and
127 the data set used for the estimation. For the purposes of this study, K_f is estimated at the European Union level,
128 so the formula chosen strikes the best balance between the accuracy of the relationship and its applicability on a
129 wide scale. Thus, the equation must:

- 130 i) Include only parameters that are measured in large soil surveys
- 131 ii) Have been fitted on a large range of each soil parameter
- 132 iii) Focus on in situ long-term contamination and not on laboratory experiments.

133

134 On December 2020 we first ran a bibliographic research on WOS looking for “Cu AND availab*AND soil AND TOPIC
135 function”. We then completed this research by examining the references cited in the articles found. We collected
136 the available relationships for estimating K_f on the basis of soil pedo-geochemical characteristics and/or total Cu.
137 We selected only relationships that were based on commonly collected soil pedo-geochemical characteristics, such
138 as soil organic matter (OM) or soil organic carbon (OC), dissolved organic carbon (DOC), cationic exchange capacity
139 (CEC), clay percentage and pH that are the most frequently reported values from large scale soil survey.

140

141 2.2 Soil data

142 This study used European data on various soil parameters, in particular pH and organic carbon (OC), obtained from
143 the Joint Research Centre's (JRC) LUCAS topsoil data. The data set is limited only to the territories of European Union
144 Member States. The aforementioned data set provides information on pH (Panagos et al., 2022; Ballabio et al.,
145 2016; ESDAC - European Commission, 2024; Panagos et al., 2012) and OC contents (Panagos et al., 2022; de Brogniez
146 et al., 2015; ESDAC - European Commission, 2024; Panagos et al., 2012)). The data has been re-gridded with cdo
147 commands (Schulzweida, 2019) to a spatial resolution of 0.5° (equivalent to approximately 50 km). This was done
148 to match the resolution of the land surface models that were used to estimate the runoff. The resulting runoff data
149 is presented in section 2.3.

150 2.3. Runoff data from land surface models

151 Runoff is computed in land models from incoming rain- and snow- falls, calculated evapotranspiration, and soil
152 hydrologic capacities. To estimate changes in soil runoff during the 21st century and to reduce uncertainties, we
153 used two typical land-surface schemes models (LSM) – namely ORCHIDEE (Krinner et al., 2005) and LPJmL (Sitch et
154 al., 2003)– and two global circulation models (GCM) providing climate projections – namely IPSL-CM5a (Dufresne
155 et al., 2013) and GDFL-ESM2m (Dunne et al., 2012) – further named CM5a and ESM2m respectively. Our study
156 exploited simulations conducted as part of the Inter-Sectoral Impact Model Intercomparison Project Phase 2b
157 (ISIMIP2b), which supplied simulations of land surface models driven by binding scenarios from 1861 to 2099 (Frieler
158 et al., 2017). Further details of the protocol used can be found at ISIMIP2b (The Inter-Sectoral Impact Model
159 Intercomparison Project, 2021) . The ISIMIP2b utilizes harmonized climate forcings derived from gridded, daily
160 bias-adjusted climate data of various CMIP5 (5th coupled model intercomparison project) global circulation models
161 (GCMs) (Frieler et al., 2017; Lange, 2016) as well as with the use of global annual atmospheric CO₂ concentration,
162 and harmonized annual land use maps (Goldewijk et al., 2017). The application of bias-corrected climate data
163 ensures that the climate used by the land surface models is consistent with observations over the last 40 years of

164 the historical period. We compared the historical data calculated by the different models with three five-year
165 periods distributed over the 21st century: 2001-2005, called historical scenario , 2051-2055 and 2091-
166 2095. In order to simulate 2051-2055 and 2091-2095 periods, we used two century-scale scenarios called
167 Representative Concentration Pathway (RCP). These scenarios have been defined by the Intergovernmental Panel
168 on Climate Change (IPCC) (van Vuuren et al., 2011) and correspond to common socio-economic pathways followed
169 by the world's population. Here, we focused on RCP 2.6, which represents an active reduction of greenhouse gas
170 emissions to comply with the Paris Agreement, and RCP 6.0, which represents more or less *business as usual*. RCP
171 2.6 is predicted to produce a radiation forcing of 2.6 W.m^{-2} , whereas RCP 6.0 would result in a radiation forcing of
172 6 W.m^{-2} .

173 For each combination of LSMs (LPJmL or ORCHIDEE) and GCMs (CM5a or ESM2m), we calculated the mean
174 over 5 years at 3 period evenly space: 2001 - 2005 , 2051 - 2055 and 2091 - 2095 of the 21st
175 century. The cross scheme of two land surface models and two GCMs enabled us to establish whether estimations
176 of runoff are influenced more by rainfall projection provided by the GCMs or the representation of soil hydrologic
177 characteristics provided by the LSMs. When predictions are driven by soil hydrologic properties, highest
178 differences in runoff predictions are expected between couple of model with the same LSM but different GCM
179 (e.g. for instance LPJmL_CM5a is closest to LPJmL_ESM2m than to ORCHIDEE_CM5a) Contrarily, when
180 predictions will be driven by rainfall projections, highest differences in runoff predictions are expected between
181 couple of model with the same GCM but different LSM (e.g. for instance LPJmL_CM5a is closest to
182 ORCHIDEE_CM5a than to LPJmL_ESM2m)

183 2.4. Assesment of AP and LP areas

184 AP or LP areas were assessed by comparing the K_f and runoff values of each grid cell with its corresponding spatial
185 median. Median runoff was computed for the whole of Europe for each five-year average period studied per
186 model. LP areas were characterized by low K_f and high runoff, while AP areas were characterized by the opposite
187 (see Eq. (3a) and (3b)). We identified grid cells with unusually high or low values, later referred as anomalies

188 as grid cells above or below a 1 MAD deviation. MAD was computed as $median(|x_i| - median(x))$, x being
 189 successively runoff and K_f for the Θ grid cells where K_f can be estimated (see Eq. (3a) and (3b)).

190 For each combination of LSM (ORCHIDEE or LPJmL) x GCM (CM5a or ESM2m) and each time period ($t=2001-2005$;
 191 2051-2055 or 2019-2095) with the two climate change scenarios (RCP 2.6 or RCP 6.0) applied for the periods 2051-
 192 2055 and 2091-2095, we have defined LP and AP areas as follows:

- 193 • Areas with soils exhibiting high potentiality of Cu leaching (LP areas) under 1 MAD threshold (named LP) for
 194 a 5 years mean time period t were defined as areas where grid cells i have:

$$195 \quad \{K_f(i) < Median(European K_f) - 1 MAD(European K_f) Runoff(t, i) >$$

$$196 \quad Median(European runoff(t)) + 1 MAD(European Runoff(t)) \} \quad (3a)$$

- 197 • Areas with soils exhibiting low potentiality of leaching corresponding to soils of high Cu accumulation potentiality
 198 (AP areas) under 1 MAD threshold (named AP) for a 5 years mean time period t were defined as areas where
 199 grid cells i have:

$$200 \quad \{K_f(i) > Median(European K_f) + 1 MAD(European K_f) Runoff(t, i) <$$

$$201 \quad Median(European runoff(t)) - 1 MAD(European Runoff(t)) \} \quad (3b)$$

202

203 The benefit of this approach is that anomalies identification is not affected by the set of coefficients
 204 chosen to compute K_f , and it removes the absolute nature of the values, but it focus on the deviation to median.
 205 .

206 We choose to calculate the MAD to each time period to emphasized the spatial variability. Anomalies
 207 identification could also be done using the historical runoff as a reference and looking at its change with time.
 208 However, when considering the actual rainfall regime as a reference, we consider that the current environmental
 209 risk well considers the spatial risk variability.

210 In the next sections the results of temporal trends are presented using median per model and mean over the 4
211 models.

212 We used R 4.1.2 (R Core Team, 2021) to compute anomalies and perform the figures.

213

214 3. Results

215 3.1. K_f estimations at the European scale

216

217 The empirical equations extracted from our literature review to estimate K_f are given in Table 1. We collected 15
218 equations allowing us to calculate K_f as the coefficient of partition between total Cu and Cu in solution. Among
219 these equations, pH was found the more decisive factor in K_f estimation (8/15 relationships). Indeed, K_f is
220 positively correlated to pH so that the more alkaline the soil is, the highest the ratio total Cu/Cu in solution is.
221 Soil organic matter (OM) or OC is less often a parameter in the K_f equations (4/15 relationships) but, when present,
222 partial slope for OM/OC is higher than that for pH which means that a small variation in soil OM content affect
223 more Cu partitioning than a small variation in pH. Three of the 4 papers concerned found a positive relationship
224 between OM and K_f while (Mondaca et al., 2015) found a negative partial slope for soil OM or dissolved OC (Table
225 1, Eq. (12d)). However, this Eq. (12d) was fitted on arid soils from Chile and includes a positive partial slope
226 for the CEC. The CEC value can be viewed as a proxy for the sum of clay and soil OM contents, so that the over
227 whole partial slope of OM is compensated in that particular situation.

228 **Table 1.: Transfer functions reviewed from literature to estimate partition coefficient of Cu. R.V stands for response variable and Int. for intercept.**
 229 **Most studies fitted K_f defined as $K_f = [Cu]_{soil}/[Cu]_{solution}^{n-opt}$ in $L.kg^{-1}$, Cu_{soil} or Cu_{tot} in $mg.kg^{-1}$, DOC (dissolved organic carbon) in $mg.L^{-1}$, OM (soil**
 230 **organic matter) in %, CEC in $cmol.kg^{-1}$, standard error around fitted coefficient are reported when indicated in the original article.**

Author	Eq	R.V	Int.	Log (Cu tot)	pH	Log (OM)	Log (DOC)	other	n-opt	R2	number of data	Range Cu tot	Range OM	Range DOC	Range pH
(Vulkan et al., 2000)	4	Log (K_f)	1.74		0.34		-0.58		1	0.42	21	19-8645		9.8-69.8	5.5-8
(Sauvé et al., 2000)	5a	Log (K_f)	1.49 ± 0.13		0.27 ± 0.02				1	0.29	447	6.8-82850			
(Sauvé et al., 2000)	5b	Log (K_f)	1.75 ± 0.12		0.21 ± 0.02	0.51 ± 0.06			1	0.42	353	6.8-82850			
(Degryse et al., 2009)	6a	Log (K_f)	0.6		0.37				1	0.34	129				
(Degryse et al., 2009)	6b	Log (K_f)	0.45		0.34			0.65 log (CEC %)	1	0.44	128				
(Unamuno et al., 2009)	7a	Log (K_f)	1.95		0.16				1	0.15	29	18-10389			
(Unamuno et al., 2009)	7b	Log (K_f)	2.383	0.46					1	0.61	29	18-10389			
(Unamuno et al., 2009)	7c	Log (K_f)	1.99	0.42	0.06				1	0.63	29	18-10389			
(Groenenberg et al., 2010)	8a	Log (K_f)	2.26		0.89	0.9			0.85	0.87	216	0.1-326	2-97.8		3.3-8.3
(Ivezić et al., 2012)	9a	Log (K_f)	3.98			0.48	-0.59		1	0.5	74	5.7-141		0.9-10.2	4.3-8.1
(Mondaca et al., 2015)	10a	Log (K_f)	1.05	0.7		-1.06			1	0.46	86	56-4441	12.0-62		6.2-7.8
(Mondaca et al., 2015)	10b	Log (K_f)	2.88	0.41			-1.03		1	0.77	86	56-4441	12.0-62		6.2-7.8
(Li et al., 2017)	11a	Log (K_f)	3.12	0.47			-0.66		1	0.28	34				
(Li et al., 2017)	11b	Log (K_f)	2.179	-0.45 * log (Cu solution) $\mu mol.L^{-1}$					1	0.42	34				
(Li et al., 2017)	11c	Log (K_f)	2.59	0.617			-1.55		1	0.88	20				

232

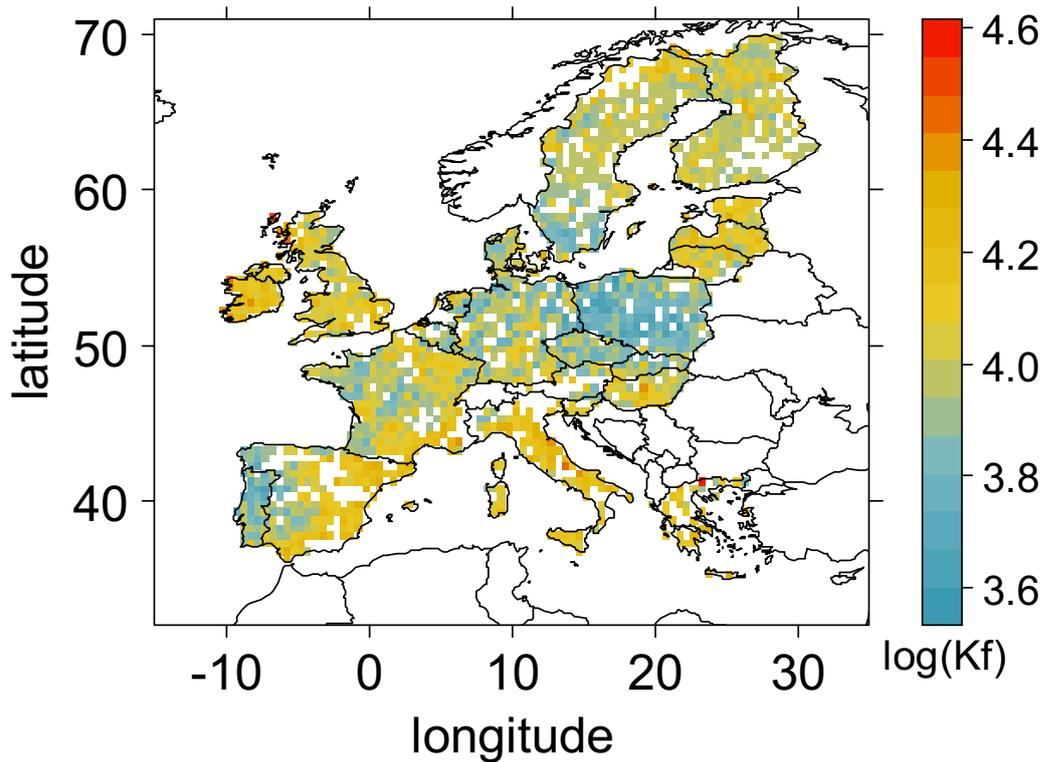
233 Over the 15 equations, the estimation of K_f according to (Sauvé et al., 2000) with Eq. (5a) or (5b) (Table 1) is the
234 most robust as determined over a wide range of soils (more than 400 points). The estimations are based on a
235 large gradient of in situ total soil Cu concentrations, even though the highest total soil Cu concentration is higher
236 than what was observed in Europe with the JR's soil survey. sSauvé et al., (2000) proposed two equations
237 based on a compilation of about 400 data points from long-term contaminated samples. One of the equations
238 considers OM values, whereas the other does not due to a lack of information in the gathered data. Finally, due
239 to the well-known importance in OM for binding with Cu, the Eq. (5b) was selected for our application at the
240 Europe scale and K_f was calculated as following:

$$241 \quad (K_f) = 1.75 + 0.21pH + 0.51(OM)$$

242 with K_f in $L.Kg^{-1}$ and OM being the soil organic matter content calculated as $OM = 2 \times OC$ from JRC following
243 (Pribyl, 2010).

244 K_f values display a range of 4600 to 21500 $L.kg^{-1}$ with a median value of 9829 $L.kg^{-1}$. K_f values below 8000 $L.kg^{-1}$
245 and above 12000 $L.kg^{-1}$ respectively represent low and high anomalies for K_f . On the European scale, a
246 heterogeneous distribution can be seen when using equation (5b), as shown in (Fig. 1).

247



248

249 Fig. 1: Map of $\log_{10}(K_f)$ in Europe at 0.5° following Eq. (5b) applied to soil Cu contents. White pixels correspond
 250 to pixel without OC measurement, and consequently no K_f estimations .

251 Beyond the E's administrative borders (e.g. Switzerland and Norway), in certain mountain areas there is a lack of
 252 OC data which is't supplied by the JRC. Cu partitioning in soil solution is low around the Mediterranean, UK, Baltic
 253 and Nordic regions with high K_f ($>12000 \text{ L.kg}^{-1}$). This accounts for 29.9 % of the grid cells, where deposited Cu can
 254 thus accumulate in soils. On the contrary, high partition of Cu into soil solution can be found in 20.1% of the grid
 255 cells where values of K_f are low ($<8000 \text{ L.kg}^{-1}$), thus providing soils with a tendency to f copper for other
 256 ecosystems, depending on the runoff. This occurs for instance near Portugal and Poland.

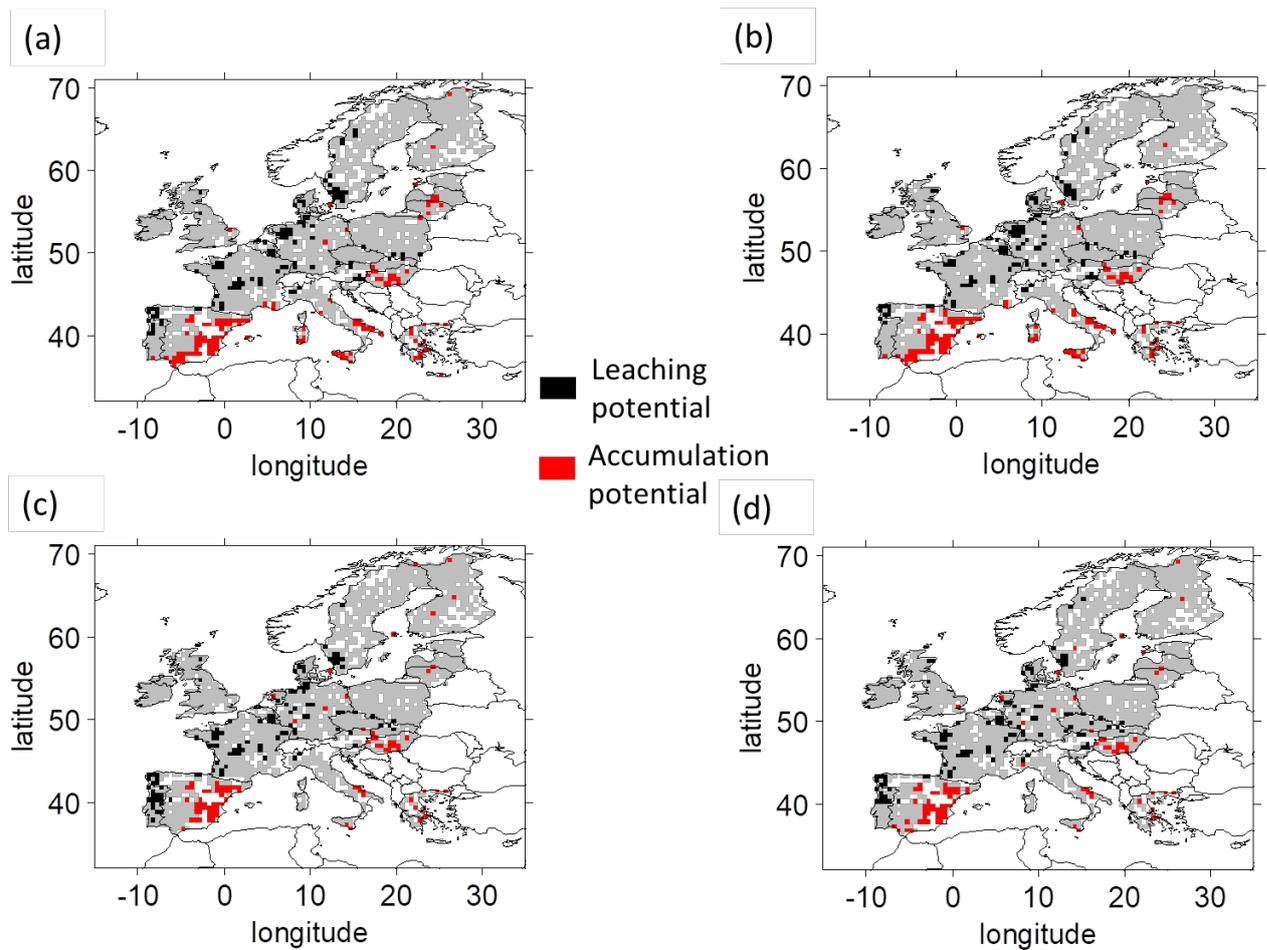
257

258 3.2. Modelling potential Cu leaching and accumulation in European soils for the historical period (2001-2005)

259 Over the two LSMs x 2 GCMs, the runoff values during the 2001-2005 period varied between 0 (LPJmL_CM5a

260 and LPJmL_ESM2m) and 5.4 mm.day^{-1} (LPJmL_CM5a). The mean runoff value over the two LSMs x 2 GCMs is 1.1
261 (± 0.1 standard deviation) mm.day^{-1} (data shown in Fig S1). For this period, the 1MAD threshold gives rather
262 similar low and high runoff anomalies between couples of LSMs x GCMs, below $0.6, 0.6, 0.7, 0.6 \text{ mm.day}^{-1}$ and
263 above $1.3, 1.2, 1.3$ and 1.1 mm.day^{-1} respectively for ORCHIDEE_CM5a, ORCHIDEE_ESM2m, LPJmL_CM5a and
264 LPJmL_ESM2m. In addition, respectively $21.7, 22.1, 20.2$ and 21.1% of the grid cells are low runoff anomalies and
265 $28.2, 27.9, 29.8$ and 28.9% of the grid cells are high runoff anomalies (see Table S1).

266 Fig. 2 represents the LP and AP areas for the 2001-2005 period and for the different combinations of LSMs
267 and GCMs. The amount of grid cells with LP and AP areas varied among the LSMs x GCMs combinations (Fig. 3
268 with the historical scenario and Table S1). However, spatial patterns are well conserved with more similarities
269 between the same LSM than between the same GCM. Globally, LP areas are located mostly in Northern Portugal
270 with scattered points around France, Germany and Scandinavia while AP areas are mostly found in South East of
271 Spain, South-Adriatic coast of Italy and scattered points in Hungary. But, with the ORCHIDEE LSM, AP areas in
272 South Spain are larger, and LP areas in France and East Europe are more scattered than with the LPJmL LSM.



273

274 Fig. 2: Areas of potential for Cu leaching (LP) and accumulation (AP) over the historical (2001-2005) period for
 275 the combinations of land surface scheme (ORCHIDEE in (a), (b) ; LPJmL in (c), (d)) and climate forcing (CM5a in (a),
 276 (c) and ESM2m in (b), (d)). White pixels correspond to pixel without OC measurement, and consequently no Kf
 277 estimations.

278

279 Over the four combinations of LSMs and GCM, LP was detected in 6.4 ± 0.1 % (median, median deviation) of
 280 the grid cells are (Fig. 3 (a)) and AP was detected in 6.7 ± 1.1 % of the grid cells (Fig. 3(b)). Areas with
 281 LP are almost equal between all LSMs x GCMs even if ESM2m forcing leads to slightly less areas with LP than
 282 CM5a. Much more AP areas are predicted by ORCHIDEE LSM. LPJmL_CM5a combination has the smallest
 283 percentage of the grid cells with AP with 5.5 %, while ORCHIDEE_CM5A has the largest percentage with 8.0
 284 % (Fig. 3(b)).

285

286

287 3.3. Modelling the changes of the LP areas over the century according to the different RCPs

288

289

290

291

292

293

294

295

296

297

298

For the two chosen climate change scenarios, median runoffs per models are expected to increase over the century for the 2 LSMs x 2 GCMs combinations. For the 2051-2055 period, predicted runoff is $1.1 \pm 0.1 \text{ mm.day}^{-1}$ with RCP 2.6 and RCP 6.0 (mean, standard deviation of the 2 LSMs x 2 GCMs over the 5 years), (see Fig. S2 for RCP 2.6 and Fig. S4 for RCP 6.0). For the 2091-2095 period, predicted runoff is also $1.1 \pm 0.1 \text{ mm.day}^{-1}$ with RCP 2.6 but $1.0 \pm 0.1 \text{ mm.day}^{-1}$ with RCP 6.0 (mean, standard deviation of the 2 LSMs x 2 GCMs over the 5 years), (Fig. S3 for RCP 2.6 and Fig. S5 for RCP 6.0). Table S1 shows that the amount of grid cells defined as high anomalies for runoff tends to decrease by the 2091-2095 period while the amount of grid cells defined as low anomalies for runoff tends to increase. However, tendencies for the 2051-2055 period are variable with in some cases an increase or a decrease in percentage by comparison with the previous or subsequent periods (see Table S1). Furthermore, among the different periods of climate change scenarios, the ratio of LP areas in percentage over areas of high anomalies for runoff is not constant (see Table S1).

299

300

301

302

303

304

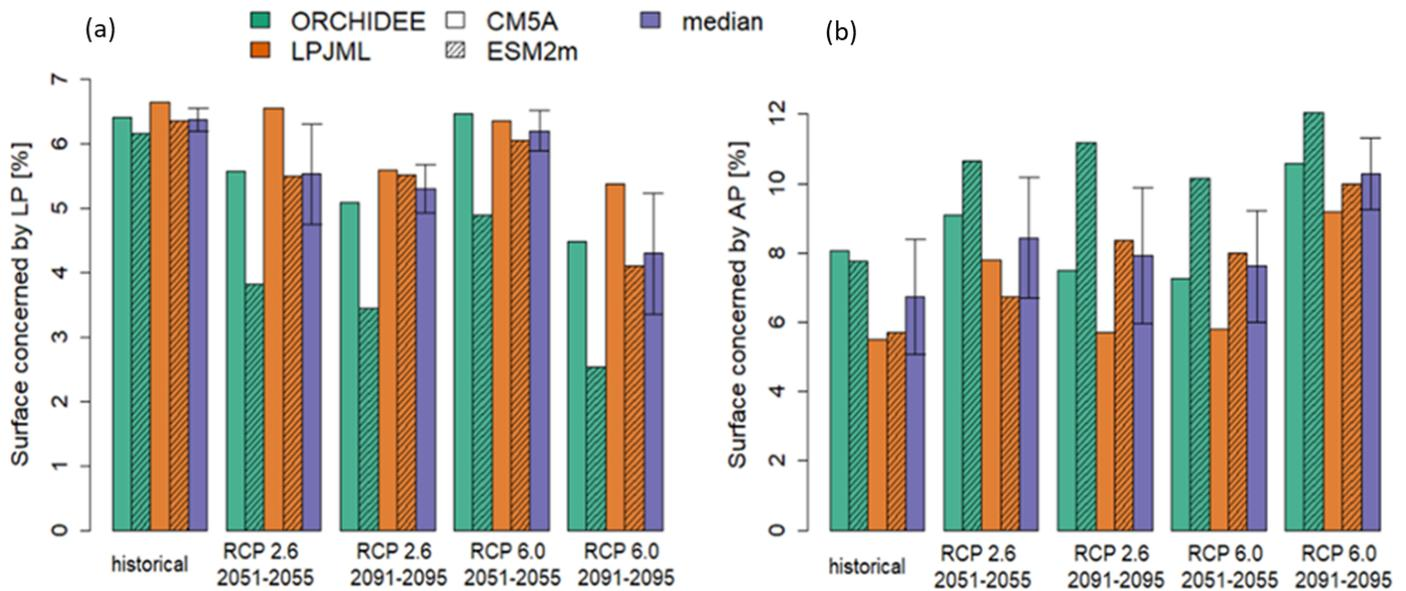
305

306

307

308

The change of areas in Europe with LP for the different climate scenarios and the different LSMs x GCMs combinations over the century is presented in percentage in Fig. 3(a). Compared to the historical values and whatever the scenario, the median percentage of grid cells with LP in 2091-2095 decreases by 1.2 ± 0.3 percentage points (median, median deviation) for RCP 2.6 and by 2.1 ± 0.5 percentage points for RCP 6.0. Hence, for the 2091-2095 period, percentage of surfaces with LP are $5.3 \pm 0.3 \%$ (median, median deviation) for RCP 2.6 and $4.3 \pm 0.6 \%$ for RCP 6.0. Areas where LP was detected are relatively similar for all the time period and climate change scenarios and for all LSMs x GCMs except ORCHIDEE_ESM2m that always predicted the smallest percentage of areas with LP. Indeed, for ORCHIDEE_ESM2m the percentage of areas with LP are from 59% (RCP 6.0 2091-2095) to 79 % (RCP 6.0 2051-2055) smallest than the median percentage of surfaces with LP (see Fig. 3(a)).



309

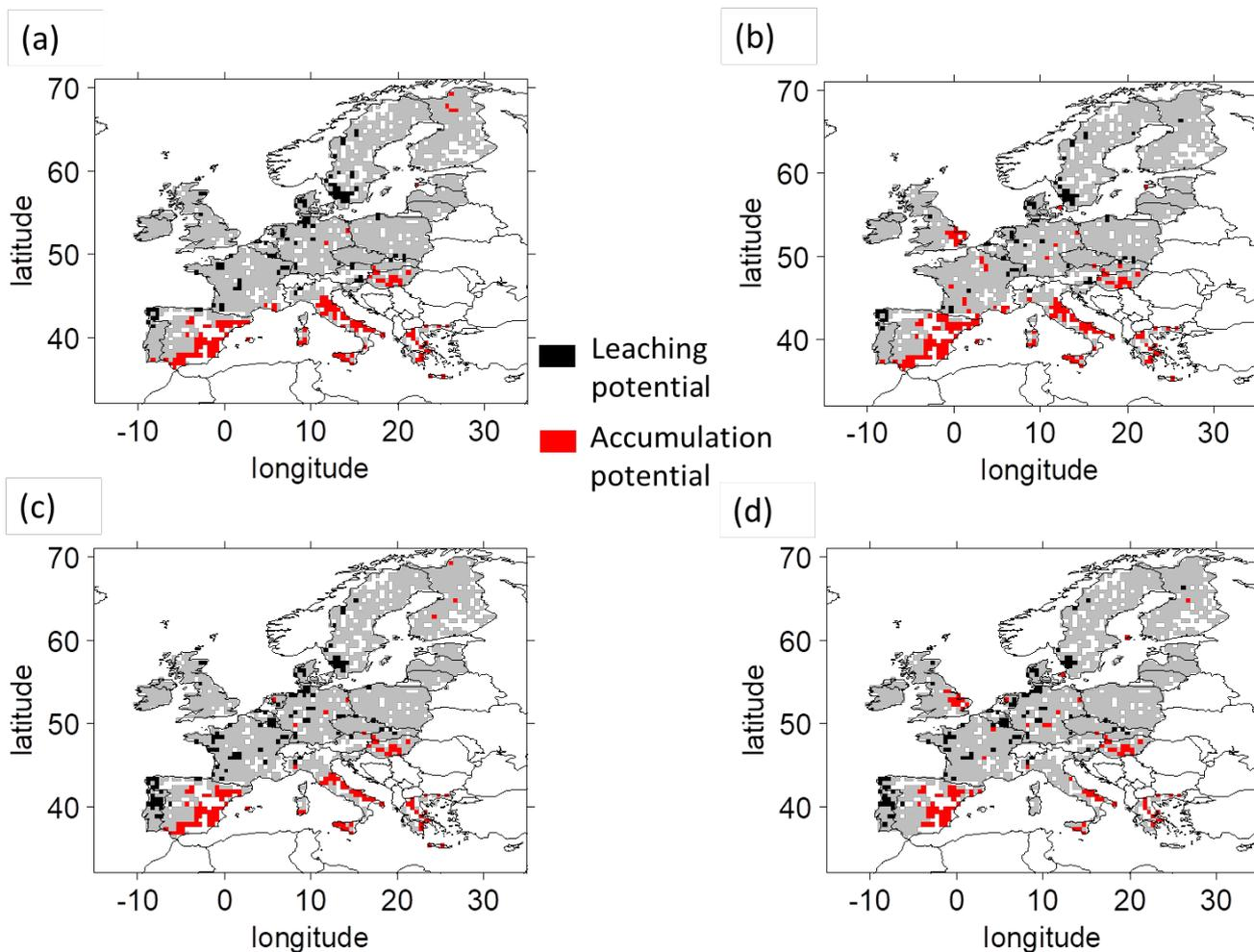
310 Fig. 3: Percentage of the grid cells with Cu LP (a) and AP (b) for the different scenarios (historical=2001-
 311 2005, RCP 2.6 horizon 2050 and 2090 and RCP 6.0 horizon 2090). The 4 combinations of the 2 LSMs (ORCHIDEE in
 312 green and LPJmL in orange) and the 2 climate forcings (CM5a fill bars and ESM2m dashed bar) as well than median
 313 (purple) of the 4 models and median deviation (bar) are plotted.

314

315 The change of LP's median during the century depends on the climate change scenario. With RCP 2.6, the
 316 median percentage of grid cells with LP varied more between the historical scenario and the 2051-2055 one ($-$
 317 0.8 ± 0.4 percentage points, median, median deviation) than between the 2051-2055 and the 2091-2095 periods
 318 (-0.4 ± 0.3 percentage points). On the contrary, with RCP 6.0, the median percentage of grid cells with LP areas
 319 decreases less from the historical scenario to the 2051-2055 one (-0.3 ± 0.2 percentage points, median, median
 320 deviation), than between the 2051-2055 and 2091-2095 periods (-2.0 ± 0.2 percentage points), see Fig. 3 (a).
 321 Furthermore, with RCP 2.6, estimations give 5.5 ± 0.5 % of the grid cells with LP in 2051-2055 and 6.2 ± 0.2 %
 322 with RCP 6.0, which is similar to the 2001-2005 estimate.

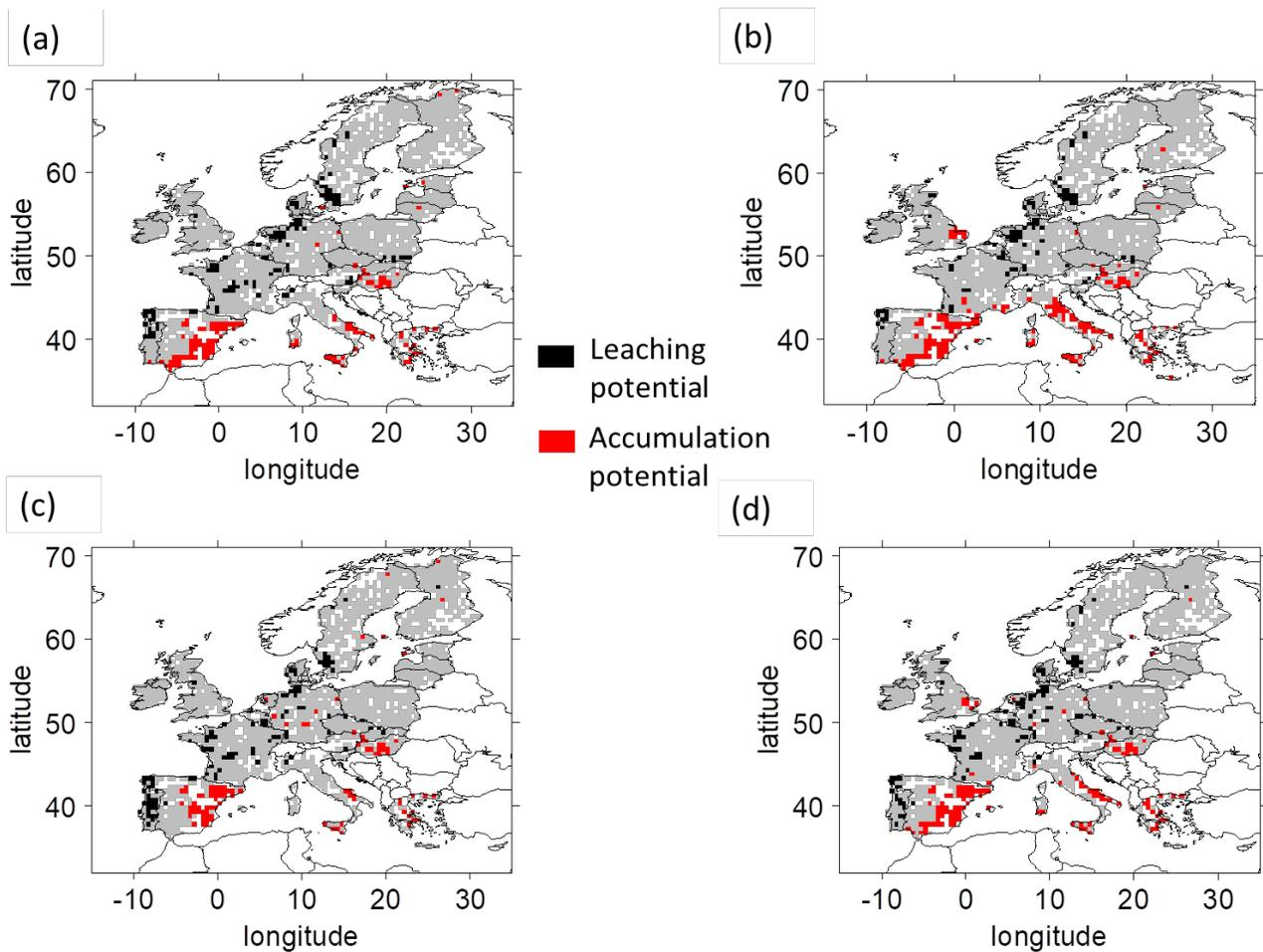
323 For all LSMs and GCMs and the two RCPs, LP areas are mostly detected in Portugal, north Germany and
 324 Scandinavia. In terms of LP risks, the combinations of GCMs and climate change scenarios mostly affect the

325 quantity of dispersed spots in East Europe and in the southern regions of Portugal. By 2050, the decrease in LP
 326 areas is mostly located in the center of France, south of Portugal and north of Germany (Fig. 4 for the RCP 2.6
 327 and Fig. 6 for the RCP 6.0). By 2090, the decrease in LP areas are mostly located in the south of Portugal (Fig.
 328 5 for the RCP 2.6 and Fig. 7 for the RCP 6.0).



329

330 Fig. 4: Areas of potential for Cu leaching (LP) and accumulation (AP) over the RCP2.6 2051-2055 period for the
 331 different combinations of land surface schemes (ORCHIDEE in (a), (b) ; LPJmL in (c), (d)) and climate forcings (CM5a
 332 in (a), (c) and ESM2m in (b), (d)). White pixels correspond to pixel without OC measurement, and consequently no
 333 Kf estimations.



334

335 Fig. 5: Areas of potential for Cu leaching (LP) and accumulation (AP) over the RCP 2.6 2091-2095 period for
 336 the different combinations of land surface schemes (ORCHIDEE in (a), (b) ; LPJmL in (c), (d)) and climate forcings
 337 (CM5a in (a), (c) and ESM2m in (b), (d)). White pixels correspond to pixel without OC measurement, and
 338 consequently no Kf estimations.

339

340 3.4. Modelling the changes of the AP areas over the century according to the different RCPs

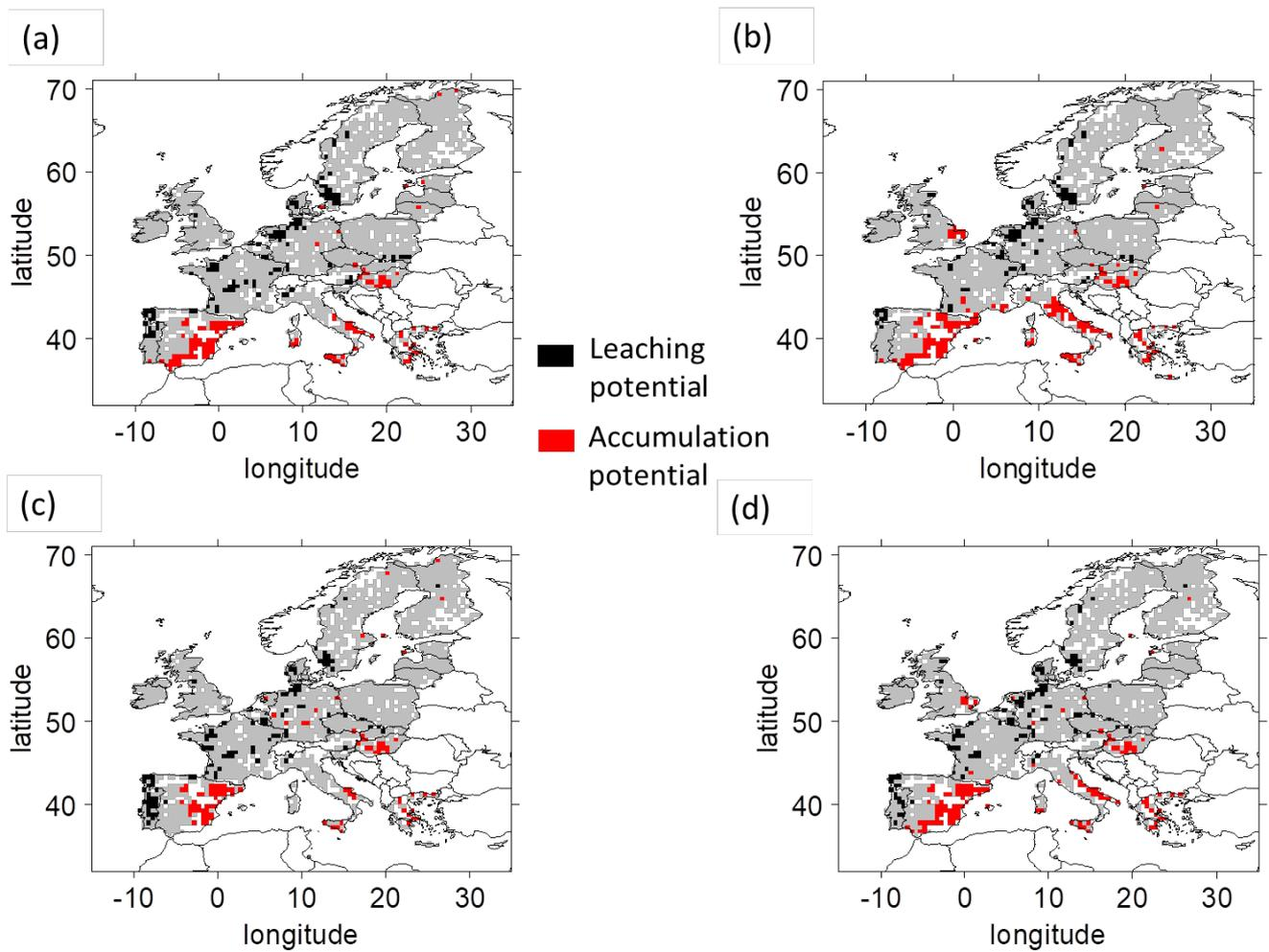
341 The change of AP areas in Europe with the different climate scenarios and the different LSMs x
 342 GCMs combination over the century is presented in percentage in Fig. 3(b). For the 2091-2095 period and for
 343 the two climate change scenarios, the percentage of grid cells an AP is detected increases for all LSMs x GCMs
 344 except for ORCHIDEE_CM5a with RCP 2.6. AP area increases are highly variable between LSMs x GCMs, with a

345 smaller increase between historical period and 2091-2095 for RCP 2.6 than for RCP 6.0.

346 With RCP 2.6, and for all LSMs x GCMs, the percentage of grid cells where an AP is detected increases
347 between the historical scenario and the 2051-2055 period. Between 2051-2055 and 2091-2095, the
348 percentage of grid cells where AP is detected increases for LSMs_ESM2m and decreases for LSMs_CM5a
349 (see Fig. 3 (b)).

350 With RCP 6.0, the percentage of areas where AP is detected increases for all LSM x GCM except with
351 ORCHIDEE_CM5a between the historical period and the 2051-2055 period, and for all LSM x GCM combinations
352 between the 2051-2055 and the 2091-2095 period.

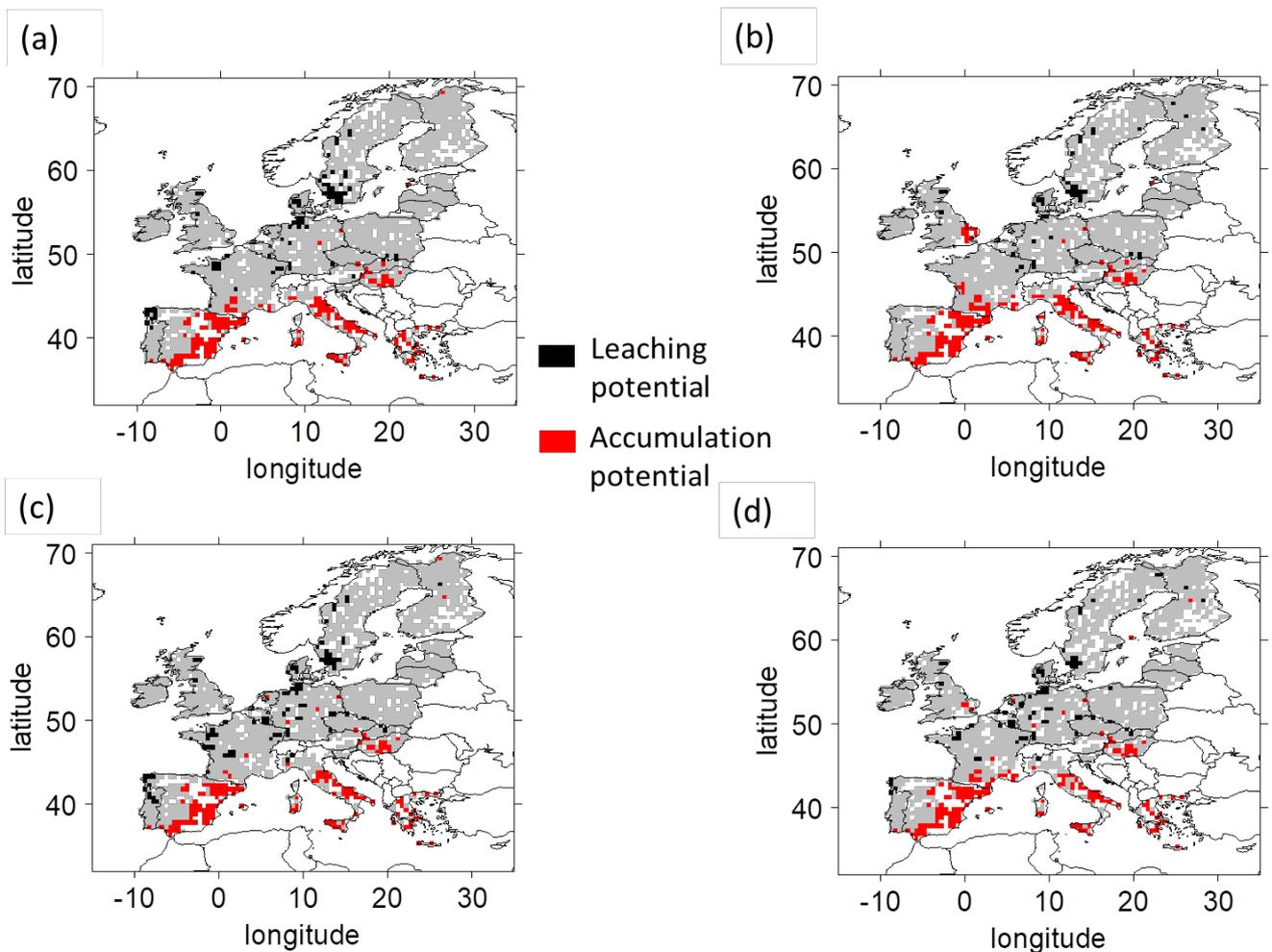
353 For all LSMs X GCMs and the two RCPs, AP areas are found in Sicilia, East Europe and South Spain. However, the
354 density and extent of the AP areas in these regions varied between LSMs x GCMs and climate change scenarios
355 (Fig. 4 and 5 for the RCP 2.6 for the 2051-2055 and by 2091-2095 periods, respectively and Fig. 6 and 7
356 for the RCP 6.0 for the 2051-2055 and by 2091-2095 periods, respectively). Over the century, we found new
357 AP areas in East Europe and Greece.



358

359 Fig. 6: Area of potential of leaching (LP) and accumulation (AP) over the RCP 6.0 2051-2055 period for the different
 360 combination of land surface scheme (ORCHIDEE in (a), (b) ; LPJmL in (c), (d)) and climate forcings (CM5a in (a), (c)
 361 and ESM2m in (b), (d)). White pixels correspond to pixel without OC measurement, and consequently no Kf
 362 estimations.

363



364

365 Fig. 7: Areas of Cu potential for leaching (LP) and accumulation (AP) potential over the RCP 6.0 2091-2095 period
 366 for the different combinations of land surface schemes (ORCHIDEE in (a), (b) ; LPJmL in (c), (d)) and climate forcings
 367 (CM5a in (a), (c) and ESM2m in (b), (d)). White pixels correspond to pixel without OC measurement, and
 368 consequently no Kf estimations.

369 Finally, over all LSMs x GCMs and climate change scenarios, the extent of areas presenting LP and AP in each
 370 region rather depends on GCM than on LSM, with more similarities between ORCHIDEE_GCM (sub figures (a) and
 371 (b) in Fig. 2, 4, 5, 6, 7) and LPJmL_GCM (sub figures (c) and (d) in Figs. 2, 4, 5, 6, 7) than between LSM_CM5a (sub
 372 figures (a) and (c) in Figs. 2, 4, 5, 6, 7) and LSM_ESM2m (sub figures (b) and (d) in Figs. 2, 4, 5, 6, 7).

373

374

375 4. Discussion

376

377 4.1. Modelling soil copper release or storage with time for contaminated soils

378 This study aims at identifying potential leaching soil areas for Cu over Europe in order to identify locations where
379 soil may play a role in the Cu transfer from soil to aquatic ecosystems. To estimate the proportion of Cu reaching
380 soil solution, we chose to focus on the partitioning coefficient K_f which is calculated based on soil properties (pH
381 and OM here) other than total soil Cu. This specific choice of K_f coefficient rather than considering only the soil
382 total Cu contents was made because Cu in solution is not strictly correlated with total Cu, nor with other single
383 soil properties as for instance pH and soil OM which are both known to affect Cu partitioning and mobility. Thus,
384 taking into account the variability of soil properties at the European scale, the spatial distribution of Cu in solution
385 was shown to be different from the spatial distribution of total Cu (Sereni et al., 2022a). However, data on Cu
386 in solution at large scales are not available making impossible the direct estimation of transport within soil
387 solution and of AP or LP areas without using the K_f . Finally, the use of partition coefficient allowed us to estimate
388 risk areas without considering total soil Cu temporal variability and with the hypothesis that pedological soil
389 characteristics will not change at the time scale studied. This is a strong implicit assumption but needed at that
390 stage. Indeed, even though some soil OM projections are available (Varney et al., 2022) to our knowledge, future
391 projections of pH values at European scale due to climate change are not available limiting our capacities to
392 calculate a time-dependent K_f . In particular, there are large uncertainties about the C stocks that may change as
393 a result of climate change and dedicated policies for increasing the C stocks (Bruni et al., 2022). Besides, organic
394 fertilizers applied to increase C stocks can change both pH and soil Cu content leading to supplementary
395 uncertainties (Laurent et al., 2020). Furthermore, together with rainfall and soil moisture changes, climate change
396 is expected to also induce higher temperatures and shorter winters, so that a shift in cultures toward the North
397 is expected (Hannah et al., 2013). Therefore, areas with currently low total soil Cu levels may potentially
398 experience a rise in Cu inputs from fungicides, which may subsequently be transported through freshwater

399 systems. Thus, the estimations of LP and AP as computed here, can be used to identify regions about to leach
400 or accumulate high amount of Cu and anticipate total content modifications that could occur with an eventual
401 change in anthropogenic activities. Indeed, land management changes due to land use changes or regulation
402 changes may affect the use of Cu in agriculture in the future with potential consequences on Cu leaching.

403 As a first step, the study conducted here could be used to highlight areas needing regulations to lower Cu input
404 thresholds. Indeed, the changes of the LP (and AP) areas we noticed are not only the reflection of the general
405 runoff change or of the current Cu risk but also underline areas of interest when combining risk linked to soil
406 contamination and climate change. For instance, in Eastern Europe, low K_f and high runoff result in Cu LP areas
407 with soils tending to transfer Cu from soils to the other ecosystems. However, in these cases, low amounts
408 of total soil Cu contents (Ballabio et al., 2018) limit the amount of Cu exports. In parallel, in Italy, we found high
409 AP areas whatever the LSMxGCM and RCP for at least one studied period and one RCP examined. In these
410 vineyard regions (Abruzzo, Marche regions), annual Cu inputs are high, resulting in Cu accumulation in soil surface
411 horizons. These high total Cu concentrations could further enter the food web (García-Esparza et al., 2006) or
412 be exported with soil particles (Imfeld et al., 2020) due to rain erosion (El Azzi et al., 2013). Highly erosive storm
413 events predicted to increase during the next decades in Europe are another risk factor for freshwater
414 contamination even in AP areas, but are often very punctual and local. Hence, to go further on, localization of
415 areas with exogenous risks of Cu dissemination have to be identified to reinforce the predictions, e.g. by coupling
416 studies of leaching potential as the one we conducted here with erosion risk studies (Panagos et al., 2021)
417 and with outlet characteristics.

418

419 4.2. Temporal change of data and scope of the modelling analysis

420 To reduce intra and inter annual variability the modelling conducted here focused on 5-years means, thus aimed
421 at smoothing seasonal variability of runoff. The K_f we calculated was not a dynamic value since we did not make
422 hypothesis about the temporal change of soil organic carbon or pH. Furthermore, K_f is defined on the

423 assumption that there is equilibrium between the solid and solution phases. This means that the amount of Cu in
424 solution estimated by this method may be less than that present immediately after Cu application and before
425 equilibrium is reached (McBride et al., 1997). Nevertheless, our results showed a good agreement between
426 the four LSMs x GCMs in their projection of the number of grid cells where both LP and AP are detected,
427 validating the use of their median to perform projections in the absence of in situ validation.

428 It must be noted that the scope of our predictions had limits that rely on the difficulties to predict whether
429 rain- and snow-falls and runoff will evolve in terms of intensity and frequency. It has already been identified
430 that during high loads events, much more Cu was transported in solution than during light events (Imfeld et al.,
431 2020) but alternations of drying and rewetting events may also affect Cu partitioning between phases
432 (Christensen and Christensen, 2003; Han et al., 2001). Also, to gain field reality at the local scale (here, up to
433 50 km) such as landscape or catchment for example, modelling will require to account for the time periods of
434 year with higher rain- and snowfalls amounts coinciding with periods of Cu use, for instance in agriculture and
435 vineyards (Ribolzi et al., 2002; Banas et al., 2010). Indeed, if intense rainfall occurs close to Cu fungicide
436 applications, a larger Cu amount than locally computed taking into account total Cu and K_f may be exported
437 through runoff (Ma et al., 2006b, a). Thus, local soil Cu budgets require the use of temporal model, which
438 accounts for the regular inputs and outputs of Cu from vegetation and runoff that cannot be accounting with
439 multiyear mean. Finally, the identification of the areas with high risks of soil Cu leaching or accumulation we made
440 in this study can be viewed as a first step for the risk change assessment of Cu contamination useful for land
441 management or Cu-fertilizer applications regulations.

442

443 5. Conclusion

444 Our approach to assess European areas with a potential to accumulate or leach copper from soils was not
445 straightforward but included several steps. We focused first on the methods to calculate Cu partitioning. By
446 reviewing existing Cu K_f 's equations we pointed out pH and soil OM contents as important determinants and more
447 precisely that the OM partial effect was larger than the pH one. Then, using the European maps of soil

448 characteristic data, we computed the map of K_f at the 0.5° scale, highlighting areas with high risk to leach or to
449 accumulate Cu for a given soil . The estimation of LP and AP areas for current and future soil runoffs under two
450 RCPs with couples of two GCMs x two LSMs was thereafter performed by comparing anomalies for both K_f and
451 runoffs We hence provided a new method to emphasize at the regional scale the combined risk of both climate
452 change and contamination. We pointed out that despite similar projections for the end of the 21st century, the
453 trend during the century depends on the climate change scenario. For the historical period (2001-2005) our
454 study showed comparable amounts of grid cells where LP or AP is detected (between [6.2% -
455 6.4%] and between [5.5% - 8.0%], respectively). During the century, AP areas were found to increase for all the
456 LSMs x GCMs and the two RCPs. On the contrary, for the two RCPs and three over the four LSMs x GCMs, LP areas
457 were found to decrease during the century compared to the current estimation. Surprisingly, the total number
458 of grid cells where AP and LP are detected in 2091-2095 is r estimated between 13.2 ± 1.3
459 (RCP 2.6) and $14.6 \pm 1.3\%$ (RCP 6.0). This was due, however, to opposite trends in the change of LP areas that
460 decrease and AP areas that increase during the century. We highlighted the areas of particular risk for
461 application of Cu, emphasizing the necessity to precise monitoring in Cu application on these areas. Future studies
462 would gained in precision by taking into account the change of partitioning coefficient with soil change or
463 scenarios of Cu application taking into account the various forms (e.g., mineral or organic fungicides).

464

465 Code availability:

466 The code can be provided upon request.

467

468 Data availability:

469 The data can be provided upon request. Soil data are available on the ESDAC (Panagos et al., 2022; ESDAC -
470 European Commission, 2024, 2012) and runoff data on ISIMIP (The Inter-Sectoral Impact Model Intercomparison
471 Project, 2021)

472

473 Credit authorships contribution statement:

474 Laura Sereni: Methodology, Formal analysis, Data processing, Writing original draft.

475 Julie-Mai Paris: Formal analysis, Initial data processing, Writing original draft.

476 Isabelle Lamy: Methodology Conceptualization, Writing review and editing, Supervision, Funding acquisition

477 Bertrand Guenet: Methodology, conceptualization, Writing review and editing, supervision, Project administration,

478

479 Declaration of competing interests

480 The authors declare that they have no known competing financial interests or personal relationships that could

481 have appeared to influence the work reported in this paper.

482

483 Acknowledgments

484 Parts of this study were financially supported by the Labex BASC through the Connexion project. LS thanks the Ecole

485 Normale Supérieure (ENS) for funding her PhD. The authors thank Nathalie de Noblet-Ducoudré for valuable

486 discussions on this paper.

487

488 Bibliography:

489

490

491 Babcsányi, I., Chabaux, F., Granet, M., Meite, F., Payraudeau, S., Duplay, J., and Imfeld, G.: Copper in soil
492 fractions and runoff in a vineyard catchment: Insights from copper stable isotopes, *Science of the Total*
493 *Environment*, 557–558, 154–162, <https://doi.org/10.1016/j.scitotenv.2016.03.037>, 2016.

494 Ballabio, C., Panagos, P., and Monatanarella, L.: Mapping topsoil physical properties at European scale using the
495 LUCAS database, *Geoderma*, <https://doi.org/10.1016/j.geoderma.2015.07.006>, 2016.

496

497 Ballabio, C., Panagos, P., Lugato, E., Huang, J. H., Orgiazzi, A., Jones, A., Fernández-Ugalde, O., Borrelli, P.,
498 and Montanarella, L.: Copper distribution in European topsoils: An assessment based on LUCAS soil
499 survey, *Science of the Total Environment*, 636, 282–298,
500 <https://doi.org/10.1016/j.scitotenv.2018.04.268>, 2018.

501 Banas, D., Marin, B., Skraber, S., Chopin, E. I. B., and Zanella, A.: Copper mobilization affected by
502 weather conditions in a stormwater detention system receiving runoff waters from vineyard soils
503 (Champagne, France), *Environmental Pollution*, 158, 476–482,
504 <https://doi.org/10.1016/j.envpol.2009.08.034>, 2010.

505 de Brogniez, D., Ballabio, C., Stevens, A., Jones, R. J. A., Montanarella, L., and van Wesemael, B.: A map of the
506 topsoil organic carbon content of Europe generated by a generalized additive model, *European Journal of Soil
507 Science*, <https://doi.org/10.1111/ejss.12193>, 2015.

508

509 Broos, K., Warne, M. S. J., Heemsbergen, D. A., Stevens, D., Barnes, M. B., Correll, R. L., and McLaughlin,
510 M. J.: Soil factors controlling the toxicity of copper and zinc to microbial processes in Australian soils,
511 *Environmental Toxicology and Chemistry*, <https://doi.org/10.1897/06-302R.1>, 2007.

512 Bruni, E., Chenu, C., Abramoff, R. Z., Baldoni, G., Barkusky, D., Clivot, H., Huang, Y., Kätterer, T., Pikuła,
513 D., Spiegel, H., Virto, I., and Guenet, B.: Multi-modelling predictions show high uncertainty of required
514 carbon input changes to reach a 4‰ target, *European J Soil Science*, 73, e13330,
515 <https://doi.org/10.1111/ejss.13330>, 2022.

516 Christensen, J. H. and Christensen, O. B.: Severe summertime flooding in Europe, *Nature*, 421, 805–806,
517 <https://doi.org/10.1038/421805a>, 2003.

518 Chu, H., Wei, J., Qiu, J., Li, Q., and Wang, G.: Identification of the impact of climate change and human
519 activities on rainfall-runoff relationship variation in the Three-River Headwaters region, *Ecological
520 Indicators*, 106, <https://doi.org/10.1016/j.ecolind.2019.105516>, 2019.

521 Degryse, F., Smolders, E., and Parker, D. R.: Partitioning of metals (Cd, Co, Cu, Ni, Pb, Zn) in soils:
522 concepts, methodologies, prediction and applications – a review, *European Journal of Soil Science*, 60,
523 590–612, <https://doi.org/10.1111/j.1365-2389.2009.01142.x>, 2009.

524 Douville, H., Raghavan, K., Renwick, J., Allan, R. P., Arias, P. A., Barlow, M., Cerezo-Mota, R., Cherchi, T.,
525 Gan, A. Y., Gergis, J., Jiang, D., Khan, A., Pokam Mba, W., Rosenfeld, D., Tierney, J., and Zolina, O.:
526 Climate Change 2021: The Physical Science Basis. Contribution of Working Group I to the Sixth
527 Assessment Report of the Intergovernmental Panel on Climate Change, in: *Fundamental and Applied
528 Climatology*, vol. 2, edited by: Masson-Delmotte, V., Zhai, P., Pirani, A., Connors, S. L., Péan, C., Berger,
529 S., Caud, N., Chen, Y., Goldfarb, L., Gomis, M. I., Huang, M., Leitzell, K., Lonnoy, E., Matthews, J. B. R.,
530 Maycock, T. K., Waterfield, T., Yelekçi, O., Yu, R., and Zhou, B., cambride university press, 13–25,

531 <https://doi.org/10.21513/2410-8758-2017-2-13-25>, 2021.

532 Dufresne, J. L., Foujols, M. A., Denvil, S., Caubel, A., Marti, O., Aumont, O., Balkanski, Y., Bekki, S.,
533 Bellenger, H., Benschila, R., Bony, S., Bopp, L., Braconnot, P., Brockmann, P., Cadule, P., Cheruy, F.,
534 Codron, F., Cozic, A., Cugnet, D., de Noblet, N., Duvel, J. P., Ethé, C., Fairhead, L., Fichet, T., Flavoni, S.,
535 Friedlingstein, P., Grandpeix, J. Y., Guez, L., Guilyardi, E., Hauglustaine, D., Hourdin, F., Idelkadi, A.,
536 Ghattas, J., Jousaume, S., Kageyama, M., Krinner, G., Labetoulle, S., Lahellec, A., Lefebvre, M. P.,
537 Lefevre, F., Levy, C., Li, Z. X., Lloyd, J., Lott, F., Madec, G., Mancip, M., Marchand, M., Masson, S.,
538 Meurdesoif, Y., Mignot, J., Musat, I., Parouty, S., Polcher, J., Rio, C., Schulz, M., Swingedouw, D., Szopa,
539 S., Talandier, C., Terray, P., Viovy, N., and Vuichard, N.: Climate change projections using the IPSL-CM5
540 Earth System Model: From CMIP3 to CMIP5, *Climate Dynamics*, [https://doi.org/10.1007/s00382-012-](https://doi.org/10.1007/s00382-012-1636-1)
541 [1636-1](https://doi.org/10.1007/s00382-012-1636-1), 2013.

542 Dunne, J. P., John, J. G., Adcroft, A. J., Griffies, S. M., Hallberg, R. W., Shevliakova, E., Stouffer, R. J.,
543 Cooke, W., Dunne, K. A., Harrison, M. J., Krasting, J. P., Malyshev, S. L., Milly, P. C. D., Phillipps, P. J.,
544 Sentman, L. T., Samuels, B. L., Spelman, M. J., Winton, M., Wittenberg, A. T., and Zadeh, N.: GFDL's ESM2
545 global coupled climate-carbon earth system models. Part I: Physical formulation and baseline simulation
546 characteristics, *Journal of Climate*, <https://doi.org/10.1175/JCLI-D-11-00560.1>, 2012.

547 El Azzi, D., Viers, J., Guiresse, M., Probst, A., Aubert, D., Caparros, J., Charles, F., Guizien, K., and Probst, J.
548 L.: Origin and fate of copper in a small Mediterranean vineyard catchment: New insights from combined
549 chemical extraction and $\delta^{65}\text{Cu}$ isotopic composition, *Science of the Total Environment*, 463–464, 91–
550 101, <https://doi.org/10.1016/j.scitotenv.2013.05.058>, 2013.

551 Elzinga, E. J., Van Grinsven, J. J. M., and Swartjes, F. A.: General purpose Freundlich isotherms for
552 cadmium, copper and zinc in soils, *European Journal of Soil Science*, 50, 139–149,
553 <https://doi.org/10.1046/j.1365-2389.1999.00220.x>, 1999.

554 ESDAC - European Commission: <https://esdac.jrc.ec.europa.eu/>, last access: 1 June 2024.

555

556 Flemming, C. A. and Trevors, J. T.: Copper toxicity and chemistry in the environment: a review, *Water,*
557 *Air, and Soil Pollution*, 44, 143–158, <https://doi.org/10.1007/BF00228784>, 1989.

558 Frieler, K., Lange, S., Piontek, F., Reyer, C. P. O., Schewe, J., Warszawski, L., Zhao, F., Chini, L., Denvil, S.,
559 Emanuel, K., Geiger, T., Halladay, K., Hurtt, G., Mengel, M., Murakami, D., Ostberg, S., Popp, A., Riva, R.,
560 Stevanovic, M., SuzGBRi, T., Volkholz, J., Burke, E., Ciais, P., Ebi, K., Eddy, T. D., Elliott, J., Galbraith, E.,
561 Gosling, S. N., Hattermann, F., Hickler, T., Hinkel, J., Hof, C., Huber, V., Jägermeyr, J., Krysanova, V.,
562 Marcé, R., Müller Schmied, H., Mouratiadou, I., Pierson, D., Tittensor, D. P., Vautard, R., Van Vliet, M.,
563 Biber, M. F., Betts, R. A., Leon Bodirsky, B., Deryng, D., Frohling, S., Jones, C. D., Lotze, H. K., Lotze-
564 Campen, H., Sahajpal, R., Thonicke, K., Tian, H., and Yamagata, Y.: Assessing the impacts of 1.5°C global
565 warming - Simulation protocol of the Inter-Sectoral Impact Model Intercomparison Project (ISIMIP2b),
566 *Geoscientific Model Development*, 10, 4321–4345, <https://doi.org/10.5194/gmd-10-4321-2017>, 2017.

567 García-Esparza, M. A., Capri, E., Pirzadeh, P., and Trevisan, M.: Copper content of grape and wine from
568 Italian farms, *Food Additives and Contaminants*, 23, 274–280,

569 <https://doi.org/10.1080/02652030500429117>, 2006.

570 Giller, K. E., Witter, E., and Mcgrath, S. P.: Toxicity of heavy metals to microorganisms and microbial
571 processes in agricultural soils: A review, *Soil Biology and Biochemistry*, 30, 1389–1414,
572 [https://doi.org/10.1016/S0038-0717\(97\)00270-8](https://doi.org/10.1016/S0038-0717(97)00270-8), 1998.

573 Goldewijk, K. K., Beusen, A., Doelman, J., and Stehfest, E.: Anthropogenic land use estimates for the
574 Holocene - HYDE 3.2, *Earth System Science Data*, 9, 927–953, <https://doi.org/10.5194/essd-9-927-2017>,
575 2017.

576 Groenenberg, J. E., Römkens, P. F. A. M., Comans, R. N. J., Luster, J., Pampura, T., Shotbolt, L., Tipping, E.,
577 and De Vries, W.: Transfer functions for solid-solution partitioning of cadmium, copper, nickel, lead and
578 zinc in soils: Derivation of relationships for free metal ion activities and validation with independent
579 data, *European Journal of Soil Science*, 61, 58–73, <https://doi.org/10.1111/j.1365-2389.2009.01201.x>,
580 2010.

581 Han, F. X., Banin, A., and Triplett, G. B.: Redistribution of heavy metals in arid-zone soils under a wetting-
582 drying cycle soil moisture regime, *Soil Science*, 166, 18–28, [https://doi.org/10.1097/00010694-](https://doi.org/10.1097/00010694-200101000-00005)
583 200101000-00005, 2001.

584 Hannah, L., Roehrdanz, P. R., Ikegami, M., Shepard, A. V., Shaw, M. R., Tabor, G., Zhi, L., Marquet, P. A.,
585 and Hijmans, R. J.: Climate change, wine, and conservation, *Proceedings of the National Academy of*
586 *Sciences of the United States of America*, 110, 6907–6912, <https://doi.org/10.1073/pnas.1210127110>,
587 2013.

588 The Inter-Sectoral Impact Model Intercomparison Project: <https://www.isimip.org/>, last access: 28 May 2021.
589

590 Imfeld, G., Meite, F., Wiegert, C., Guyot, B., Masbou, J., and Payraudeau, S.: Do rainfall characteristics
591 affect the export of copper, zinc and synthetic pesticides in surface runoff from headwater catchments?,
592 *Science of the Total Environment*, 741, 140437, <https://doi.org/10.1016/j.scitotenv.2020.140437>, 2020.

593 Ivezić, V., Almås, Å. R., and Singh, B. R.: Predicting the solubility of Cd, Cu, Pb and Zn in uncontaminated
594 Croatian soils under different land uses by applying established regression models, *Geoderma*, 170, 89–
595 95, <https://doi.org/10.1016/j.geoderma.2011.11.024>, 2012.

596 Komárek, M., Čadková, E., Chrastný, V., Bordas, F., and Bollinger, J. C.: Contamination of vineyard soils
597 with fungicides: A review of environmental and toxicological aspects, *Environment International*, 36,
598 138–151, <https://doi.org/10.1016/j.envint.2009.10.005>, 2010.

599 Krinner, G., Viovy, N., de Noblet-Ducoudré, N., Ogée, J., Polcher, J., Friedlingstein, P., Ciais, P., Sitch, S.,
600 and Prentice, I. C.: A dynamic global vegetation model for studies of the coupled atmosphere-biosphere
601 system, *Global Biogeochemical Cycles*, <https://doi.org/10.1029/2003GB002199>, 2005.

602 Lange, S.: Earth2Observe, WFDEI and ERA-Interim data Merged and Bias-corrected for ISIMIP (EWEMBI),
603 GFZ Data Services, 2016.

604 Laurent, C., Bravin, M. N., Crouzet, O., Pelosi, C., Tillard, E., Lecomte, P., and Lamy, I.: Increased soil pH

605 and dissolved organic matter after a decade of organic fertilizer application mitigates copper and zinc
606 availability despite contamination, *Science of the Total Environment*,
607 <https://doi.org/10.1016/j.scitotenv.2019.135927>, 2020.

608 Li, B., Ma, Y., and Yang, J.: Is the computed speciation of copper in a wide range of Chinese soils
609 reliable?, *Chemical Speciation and Bioavailability*, 29, 205–215,
610 <https://doi.org/10.1080/09542299.2017.1404437>, 2017.

611 Ma, Y., Lombi, E., Oliver, I. W., Nolan, A. L., and McLaughlin, M. J.: Long-term aging of copper added to
612 soils, *Environmental Science and Technology*, 40, 6310–6317, <https://doi.org/10.1021/es060306r>,
613 2006a.

614 Ma, Y., Lombi, E., Nolan, A. L., and McLaughlin, M. J.: Short-term natural attenuation of copper in soils:
615 Effects of time, temperature, and soil characteristics, *Environmental Toxicology and Chemistry*, 25, 652–
616 658, <https://doi.org/10.1897/04-601R.1>, 2006b.

617 McBride, M., Sauvé, S., and Hendershot, W.: Solubility control of Cu, Zn, Cd and Pb in contaminated
618 soils, *European Journal of Soil Science*, 48, 337–346, <https://doi.org/10.1111/j.1365->
619 2389.1997.tb00554.x, 1997.

620 Mimikou, M. A., Baltas, E., Varanou, E., and Pantazis, K.: Regional impacts of climate change on water
621 resources quantity and quality indicators, *Journal of Hydrology*, 234, 95–109,
622 [https://doi.org/10.1016/S0022-1694\(00\)00244-4](https://doi.org/10.1016/S0022-1694(00)00244-4), 2000.

623 Mondaca, P., Neaman, A., Sauvé, S., Salgado, E., and Bravo, M.: Solubility, partitioning, and activity of
624 copper-contaminated soils in a semiarid region, *Journal of Plant Nutrition and Soil Science*, 178, 452–
625 459, <https://doi.org/10.1002/jpln.201400349>, 2015.

626 Noll, M. R.: Trace Elements in Terrestrial Environments, 374–374 pp.,
627 <https://doi.org/10.2134/jeq2002.3740>, 2003.

628 Panagos, P., Van Liedekerke, M., Jones, A., and Montanarella, L.: European Soil Data Centre: Response to
629 European policy support and public data requirements, *Land Use Policy*, 29, 329–338,
630 <https://doi.org/10.1016/j.landusepol.2011.07.003>, 2012.

631

632 Panagos, P., Ballabio, C., Himics, M., Scarpa, S., Matthews, F., Bogonos, M., Poesen, J., and Borrelli, P.:
633 Projections of soil loss by water erosion in Europe by 2050, *Environmental Science and Policy*, 124, 380–
634 392, <https://doi.org/10.1016/j.envsci.2021.07.012>, 2021.

635 Panagos, P., Van Liedekerke, M., Borrelli, P., Köninger, J., Ballabio, C., Orgiazzi, A., Lugato, E., Liakos, L., Hervas, J.,
636 Jones, A., and Montanarella, L.: European Soil Data Centre 2.0: Soil data and knowledge in support of the EU,
637 *European J Soil Science*, 73, e13315, <https://doi.org/10.1111/ejss.13315>, 2022.

638

639 Pribyl, D. W.: A critical review of the conventional SOC to SOM conversion factor, *Geoderma*, 156, 75–
640 83, <https://doi.org/10.1016/j.geoderma.2010.02.003>, 2010.

641 R Core Team: R core team (2021), R: A language and environment for statistical computing. R
642 Foundation for Statistical Computing, Vienna, Austria. URL <http://www.R-project.org>, ISBN 3-900051-
643 07-0, URL <http://www.R-project.org/>, 2021.

644 Ribolzi, O., Valles, V., Gomez, L., and Voltz, M.: Speciation and origin of particulate copper in runoff
645 water from a Mediterranean vineyard catchment, *Environmental Pollution*, 117, 261–271,
646 [https://doi.org/10.1016/S0269-7491\(01\)00274-3](https://doi.org/10.1016/S0269-7491(01)00274-3), 2002.

647 Rooney, C. P., Zhao, F. J., and McGrath, S. P.: Soil factors controlling the expression of copper toxicity to
648 plants in a wide range of European soils, *Environmental Toxicology and Chemistry*, 25, 726–732,
649 <https://doi.org/10.1897/04-602R.1>, 2006.

650 Salminen, R. and Gregorauskiene, V.: Considerations regarding the definition of a geochemical baseline
651 of elements in the surficial materials in areas differing in basic geology, *Applied Geochemistry*,
652 [https://doi.org/10.1016/S0883-2927\(99\)00077-3](https://doi.org/10.1016/S0883-2927(99)00077-3), 2000.

653 Sauv e, S., Hendershot, W., and Herbert E., A.: Solid-Solution Partitioning of Metals in Contaminated
654 Soils: Dependence on pH, Total Metal Burden, and Organic Matter, *American Chemical Society*, 1125–
655 1131, <https://doi.org/10.1021/es9907764>, 2000.

656 Schulzweida, U.: CDO User Guide, , <https://doi.org/10.5281/zenodo.2558193>, 2019.

657 Sereni, L., Guenet, B., and Lamy, I.: Mapping risks associated with soil copper contamination using
658 availability and bio-availability proxies at the European scale, *Environmental Science and Pollution*
659 *Research*, <https://doi.org/10.1007/s11356-022-23046-0>, 2022a.

660 Sitch, S., Smith, B., Prentice, I. C., Arneeth, A., Bondeau, A., Cramer, W., Kaplan, J. O., Levis, S., Lucht, W.,
661 Sykes, M. T., Thonicke, K., and Venevsky, S.: Evaluation of ecosystem dynamics, plant geography and
662 terrestrial carbon cycling in the LPJ dynamic global vegetation model, *Global Change Biology*,
663 <https://doi.org/10.1046/j.1365-2486.2003.00569.x>, 2003.

664 Unamuno, V. I. R., Meers, E., Du Laing, G., and Tack, F. M. G.: Effect of physicochemical soil
665 characteristics on copper and lead solubility in polluted and unpolluted soils, *Soil Science*, 174, 601–610,
666 <https://doi.org/10.1097/SS.0b013e3181bf2f52>, 2009.

667 Varney, R. M., Chadburn, S. E., Burke, E. J., and Cox, P. M.: Evaluation of soil carbon simulation in CMIP6
668 Earth system models, *Biogeosciences*, <https://doi.org/10.5194/bg-19-4671-2022>, 2022.

669 Vidal, M., Santos, M. J., Abr o, T., Rodr guez, J., and Rigol, A.: Modeling competitive metal sorption in a
670 mineral soil, *Geoderma*, 149, 189–198, <https://doi.org/10.1016/j.geoderma.2008.11.040>, 2009.

671 Vulkan, R., Zhao, F. J., Barbosa-Jefferson, V., Preston, S., Paton, G. I., Tipping, E., and McGrath, S. P.:
672 Copper speciation and impacts on bacterial biosensors in the pore water of copper-contaminated soils,
673 *Environmental Science and Technology*, 34, 5115–5121, <https://doi.org/10.1021/es0000910>, 2000.

674 van Vuuren, D. P., Edmonds, J., Kainuma, M., Riahi, K., Thomson, A., Hibbard, K., Hurtt, G. C., Kram, T.,
675 Krey, V., Lamarque, J. F., Masui, T., Meinshausen, M., Nakicenovic, N., Smith, S. J., and Rose, S. K.: The
676 representative concentration pathways: An overview, *Climatic Change*, 109, 5–31,

677 <https://doi.org/10.1007/s10584-011-0148-z>, 2011.

678 West, T. S. and Coombs, T. L.: Soil as the Source of Trace Elements [and Discussion], Philosophical
679 Transactions of the Royal Society of London. Series B, Biological Sciences, 294, 19–39, 1981.

680